EBioMedicine 65 (2021) 103218

Contents lists available at ScienceDirect

EBioMedicine

journal homepage: www.elsevier.com/locate/ebiom

Research paper

Profiling of conditionally reprogrammed cell lines for *in vitro* chemotherapy response prediction of pancreatic cancer

Hee Seung Lee[a,1,2], Eunyoung Kim[b,1,2], Jinyoung Lee[a], Seung Joon Park[c], Ho Kyoung Hwang[d], Chan Hee Park[a], Se-Young Jo[b], Chang Moo Kang[d], Seung-Mo Hong[e], Huapyong Kang[a], Jung Hyun Jo[a], In Rae Cho[a], Moon Jae Chung[a], Jeong Youp Park[a], Seung Woo Park[a], Si Young Song[a], Jung Min Han[c,f], Sangwoo Kim[b,*], Seungmin Bang[a,*]

[a] *Division of Gastroenterology, Department of Internal Medicine, Yonsei University College of Medicine, 50-1 Yonsei-ro, Seodaemun-gu, Seoul 03722, South Korea*
[b] *Department of Biomedical Systems Informatics and Brain Korea 21 PLUS Project for Medical Science, Yonsei University College of Medicine, 50-1 Yonsei-ro, Seodaemun-gu, Seoul 03722, South Korea*
[c] *Department of Integrated OMICS for Biomedical Science, Yonsei University, Seoul 03722, South Korea*
[d] *Department of Surgery, Yonsei University College of Medicine, Seoul, South Korea*
[e] *Department of Pathology, University of Ulsan College of Medicine, Asan Medical Center, Seoul, South Korea*
[f] *Yonsei Institute of Pharmaceutical Sciences, College of Pharmacy, Yonsei University, Incheon 21983, South Korea*

ARTICLE INFO

Article History:
Received 4 May 2020
Revised 5 January 2021
Accepted 7 January 2021
Available online xxx

Keywords:
Pancreatic ductal adenocarcinoma
Conditionally reprogrammed cell lines
Next-generation sequencing
Patient-derived cancer cell line
Precision medicine

ABSTRACT

Background: The establishment of patient-derived models for pancreatic ductal adenocarcinoma (PDAC) using conventional methods has been fraught with low success rate, mainly because of the small number of tumour cells and dense fibrotic stroma. Here, we sought to establish patient-derived model of PDAC and perform genetic analysis with responses to anticancer drug by using the conditionally reprogrammed cell (CRC) methodology.
Methods: We performed *in vitro* and *in vivo* tumourigenicity assays and analysed histological characteristics by immunostaining. We investigated genetic profiles including mutation patterns and copy number variations using targeted deep sequencing and copy-number analyses. We assessed the responses of cultured CRCs to the available clinical anticancer drugs based on patient responsiveness.
Findings: We established a total of 28 CRCs from patients. Of the 28 samples, 27 showed *KRAS* mutations in codon 12/13 or codon 61. We found that somatic mutations were shared in the primary-CRC pairs and shared mutations included key oncogenic mutations such as *KRAS* (9 pairs), *TP53* (8 pairs), and *SMAD4* (3 pairs). Overall, CRCs preserved the genetic characteristics of primary tumours with high concordance, with additional confirmation of low-AF *NPM1* mutation in CRC (35 shared mutations out of 36 total, concordance rate=97.2%). CRCs of the responder group were more sensitive to anticancer agents than those of the non-responder group ($P < 0.001$).
Interpretation: These results show that a pancreatic cancer cell line model can be efficiently established using the CRC methodology, to better support a personalized therapeutic approach for pancreatic cancer patients.
Funding: 2014R1A1A1006272, HI19C0642-060019, 2019R1A2C2008050, 2020R1A2C209958611, and 2020M3E5E204028211

1. Introduction

Pancreatic ductal adenocarcinoma (PDAC) has the worst prognosis among all cancers, with an overall 5-year survival of approximately 10%, and it is expected to become the second leading cause of cancer deaths by 2030 [1]. Even in patients who undergo complete resection, long-term survival is poor owing to tumour recurrence [2].

Studies on many types of cancers have shown that next-generation sequencing (NGS)-based genomic analysis sheds light on profiling of genetic aberrations, identification of novel therapeutic targets and clinical practices for personalized treatment that remarkably increase survival [3–6]. Unlike other cancers, however, these applications have been largely limited in PDAC because of the difficulty in obtaining sufficient amount of high quality specimens, owing to the

* Corresponding authors.
E-mail addresses: swkim@yuhs.ac (S. Kim), bang7028@yuhs.ac (S. Bang).
[1] These authors contributed equally to this work.
[2] These authors are co-first authors.

https://doi.org/10.1016/j.ebiom.2021.103218

Research in context

Evidence before this study

Pancreatic ductal adenocarcinoma is one of the most aggressive malignancies. Next-generation sequencing-based genomic analyses and genetic aberration profiling have been employed for many tumour types to identify novel therapeutic targets. However, in most cases, only small amounts of biopsy specimens are available for analysis. To address these problems, various conventional preclinical cancer models are being developed. This strategy has been largely limited in pancreatic ductal adenocarcinoma because of the difficulty in obtaining sufficient amounts of high-quality specimens, owing to the low eligibility of the patients for surgery due to rapid disease progression, and the predominance of stromal cells in the tumour.

Added value of this study

We rapidly established patient-derived pancreatic cancer cell lines from tumour samples and then performed genetic analyses using these cells. We found that somatic mutations were maintained in cell lines and shared mutations included key oncogenic mutations such as *KRAS, TP53*, and *SMAD4*. Overall, patient-derived cell lines preserved the genetic characteristics of the primary tumours with high concordance. Cells can be isolated from patients at all stages of pancreatic cancer using the limited tissue available from a fine needle tumor biopsy as the starting tissue. Furthermore, *ex-vivo* examination of patient-derived cell lines revealed drug responsiveness predictions, which matched the clinical results.

Implications of all the available evidence

Our findings suggest that patient-specific preclinical cancer cell lines can be efficiently established and maintain original tumour characteristics. These matched patient-derived cells might support a personalized therapeutic approach for pancreatic adenocarcinoma.

low eligibility of patients for surgery because of the rapid disease progression, and the predominance of stromal cells in the tumour [7]. Hence, in most cases, only small amounts of biopsy specimens are available for analysis. To address these problems, various preclinical cancer models have been developed including cancer cell line models and patient-derived xenografts [8,9]. However, reduced stability, high cost, and lengthy preparation time hindered their active use in PDAC, emphasizing the immediate requirement of a more efficient model.

Recently, a new technique that establishes patient-derived cell lines without the use of extrinsic genetic immortalization, named "conditional reprogramming" (CR) enabled rapid and stable cell culture [10]. The conditionally reprogrammed cells (CRCs)—patient-derived tumour cells generated by CR—could be grown indefinitely under defined conditions and the karyotype was maintained even after numerous passages [11–15]. Moreover, the entire procedure can be started with a very small amount of primary tissue (~5 mm), such as biopsy specimens. Considering these benefits, we assumed that CR could be used as a beneficial platform for applying genomic analysis and predicting patient response in PDAC.

Here, using the CRC methodology, we aimed to develop PDAC cell lines that phenotypically represent primary human PDAC specimens and to identify patient-derived cell line models that can predict patient therapeutic responses in pancreatic cancer.

2. Methods

2.1. Patients and tissue samples

Patients diagnosed with PDAC were enrolled for establishment of the tumour model and genetic analysis. Tumour specimens ($\leq$1 cm) were obtained from the resected tissues of patients who underwent surgery for PDAC. For patients with unresectable PDAC, endoscopic ultrasound (EUS)-guided biopsy or percutaneous biopsy was performed to obtain the tumour specimens (Fig. 1). Tumour tissues and paired peripheral blood samples were collected simultaneously. All tissues were placed in a medium containing antibiotics. Using forceps and a scalpel, the residual fat tissue was removed. Tumour tissues were minced into 1–2 mm small fragments with sterile scissors. Dissected specimens were placed in the medium. Primary cells were isolated within 1–2 h of tumour resection. If the specimens could not be processed immediately to prepare CRCs, the tumour tissues were frozen in liquid nitrogen for long-term storage.

2.2. Ethics

This study was approved by the Institutional Review Board of Severance Hospital, Seoul, South Korea (No. 4-2015-0297). Written informed consent was obtained from all patients for sample collection and molecular analysis. All experiments were performed in accordance with the relevant guidelines.

2.3. Conditionally reprogrammed cell line culture and cell characterization

The experimental procedure was performed as described previously [10,11,14,16]. Cells were characterized by immunofluorescence and Soft agar colony formation assay, and tumourigenicity was evaluated according to the manufacturer's protocol.

2.3.1. Conditionally reprogrammed cell lines

The tissue was re-suspended in collagenase (1 mg/mL, Sigma, St. Louis, MO, USA) in culture medium and incubated for 30 min at 37°C with agitation to dissociate the tumour tissue from the collagenous stroma. We added 5x F medium for neutralization, followed by centrifugation at 1500 rpm for 3 min. The supernatant was filtered through a cell strainer (70 μm nylon, Falcon). The filtered tumour cells were seeded on a feeder layer of lethally irradiated (30 Gy) J2 murine fibroblasts in F medium. The F medium consisted of 70% Ham's F-12 nutrient mix (Hyclone, Logan, UT, USA) and 25% complete Dulbecco's modified Eagle's medium, supplemented with 0.4 μg/mL hydrocortisone (Sigma), 5 μg/mL insulin, 8.4 ng/mL cholera toxin (Sigma-Aldrich, St. Louis, MO, USA), 10 ng/mL epidermal growth factor, 5% fetal bovine serum (Hyclone), 24 μg/mL adenine (Sigma), 10 μg/mL gentamycin (Life Technologies), and 250 ng/mL Amphotericin B (Thermo Fisher Scientific, Waltham, MA, USA). Cells were cultured in the presence of the Rho-associated kinase (ROCK) inhibitor, Y-27632 at a final concentration of 5 μM (Enzo Life Sciences, Farmingdale, NY, USA). Cells were incubated at 37°C in a humidified atmosphere with 5% CO_2. Tumour cells on the plates were visibly apparent by morphology relative to stromal cells (e.g., fibroblasts). Contaminating stromal cells were removed by differential trypsinization or selective scraping of the plates as necessary. The cell lines were pretreated with 500 ng/mL mycoplasma removal agent (MP Biomedicals, Santa Ana, CA, USA). The generated cell lines were regularly checked to ensure that they were not infected with mycoplasma.

2.3.2. Immunofluorescence assay

Cells were fixed in 4% paraformaldehyde for 15 min at room temperature (RT) and washed three times with PBS, followed by blocking with 5% normal goat serum for 1 h and incubation with primary

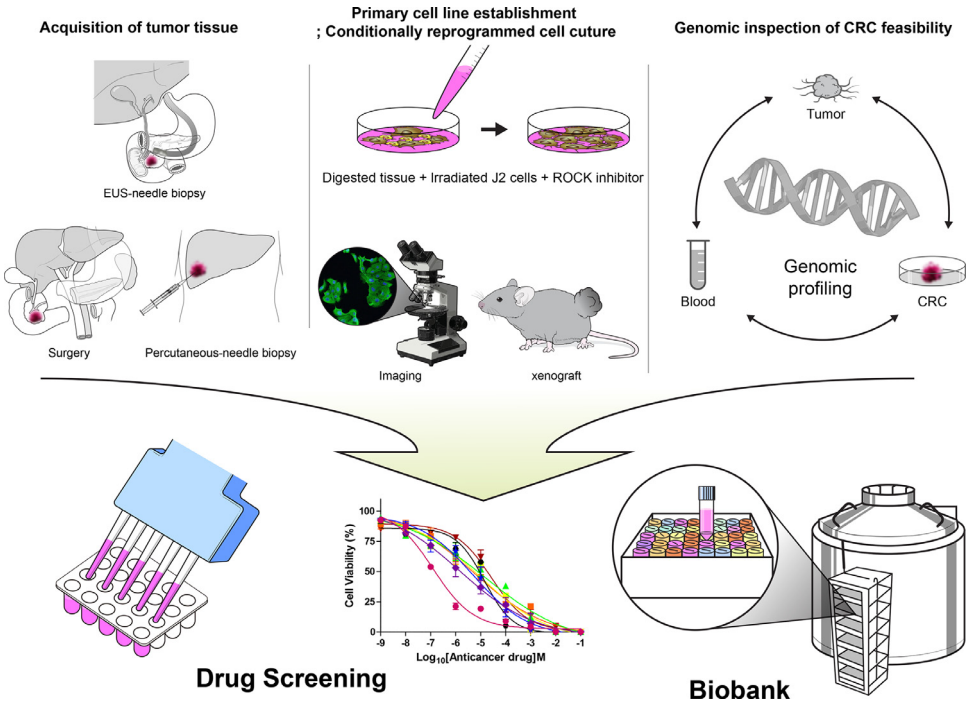

Fig. 1. Process flow chart. Tumour specimens were obtained from resected tissues of patients who underwent surgery for pancreatic ductal adenocarcinoma (PDAC). For patients with unresectable PDAC, endoscopic ultrasound-guided biopsy or percutaneous biopsy was performed to obtain the tumour specimens. Tissue samples were co-cultured with J2 murine fibroblast feeder cells and medium containing the Rho−kinase inhibitor (Y−27632). We validated the genetic similarity of established conditionally reprogrammed cell lines by comparing their 83 targeted gene sequences with that of original PDAC tissue. Finally, a drug screening platform and a biobank of human PDAC cell lines were generated by using conditional reprogramming methodology.

antibodies at room temperature (1 h). The cells were then washed three times with PBS, and incubated with secondary antibody for 30 min. The following primary antibodies were used: a-Amylase (sc−25562, rabbit polyclonal; Santa Cruz Biotechnology, dilution 1:100), cytokeratin 19 (A53-B/A2: sc-6278, mouse monoclonal; Santa Cruz Biotechnology, dilution 1:100), insulin (sc−8033, mouse monoclonal; Santa Cruz Biotechnology, dilution 1:100), and vimentin (D21H3: #5741, mouse monoclonal; Cell signaling technology, dilution 1:100). The cells were stained using Alexa Flour-conjugated secondary antibodies from Invitrogen.

3.3.3. Soft agar colony formation assay

To evaluate tumourigenicity, *in vitro* tumourigenesis and anchorage-independent growth of CRCs were evaluated by colony formation assay in soft agar. Soft agar colony formation assays were performed using the double-layer soft agar method. In each well of a 6-well plate, 5×10^4 cells were plated on the top agar (0.5% agarose gel) over a base agar (1% agarose gel). After 2-3 weeks of incubation in soft agar, the average number of colonies formed by CRCs were quantitated.

3.3.4. KRAS mutation analysis by polymerase chain reaction (PCR)

KRAS mutations were analysed by PCR. The methods used to evaluate *KRAS* mutations are essentially divided into sequencing and PCR-based techniques. Sequencing might lack sensitivity, particularly in the presence of large amounts of wild-type DNA from infiltrating cells, while PCR-based methods often show better sensitivity. Genetic analysis of the *KRAS* gene was performed by PCR amplification of exon 1 (codon 12, 13 and 61), followed by direct sequencing of the PCR products. DNA was extracted using QIAGEN QIAamp® DNA Mini Kit (Hilden, Germany). PCR primers used for *KRAS* sequencing were as follows: forward, 5′−aggcctgctgaaaatgactga−3′; and reverse, 5′−ggtcctgcac cagtaatatgca −3′ (length: 164 bp).

3.4. Immunofluorescence staining for tissue slide

Immunostaining was performed on paraffin-embedded human pancreatic cancer tissues with antibody to S100A2 (#S6797, sigma-aldrich), GATA6 (#AF1700, R&D systems) and esophagus cancer tissue was using GATA6 negative control. The paraffin-embedded slides were deparaffinized by immersion three times in xylene for 5 min. Rehydrate were performed two times 100% EtOH for 5 min, 95% EtOH for 5 min and 90%~30% EtOH for 1min followed by washes two times with H2O for 5 min. Antigen retrieval was performed 0.01 M citrate buffer (pH 6.0) in boiled water bath for 30 minutes and slides were allowed to step-down cooling in the same buffer for 30 min. Endogenous peroxidase activity was blocked 0.3% H2O2 with MeOH at room temperature for 20 minutes. Slides were then incubated with 10% normal horse serum and 0.2% Triton X-100 for 1 hour to reduce background non-specific staining and permeabilized the tissues, followed by three times washing with PBS buffer for 5 min. Each slides was incubated in first primary antibody GATA6 (10 ug/ml) overnight at 4°C. After washing three times, slides were incubated with secondary antibody Alexa Fluor 594 (1:400, Invitrogen) for 1 hr at room temperature. After washing three times, the subsequent reaction was repeated blocking step. Blocked slides were incubated in second primary antibody S100A2 (1:500) for 1 hr at room temperature. After washing three times, slides were incubated secondary antibody Alexa Fluor 488 (1:400, Invitrogen) for 1 hr at room temperature. After three times washing, the slides were mounted using anti-fade mounting solution contained with DAPI (H-1200, vector Laboratories Inc. Burlingame, CA 94010). The immunofluorescence images were acquired Olympus BF53 microscopy and the signal intensity of each image was analysed using ImageJ analysis software (NIH).

3.5. Targeted deep sequencing and RNA sequencing

We validated the genetic similarity of the established CRCs with the original PDAC tissue by comparing 83 targeted gene sequences to develop representative genomic data of PDAC (Supplementary Table 1). Targeted sequencing was performed using the Cancer-SCAN panel (83-gene panel at ~900 ×) [17]. Initially, DNA obtained by the microdissection of formalin-fixed paraffin-embedded PDAC tissue and DNA from pancreatic CRCs of the same patient were sequenced. DNA was extracted using the QIAamp DNA Mini Kit and sequenced using a HiSeq2500 system (Illumina, San Diego, CA, USA). Quality of the DNA was evaluated using a Nanodrop spectrophotometer (Thermo Fisher Scientific). Preprocessing of read sequences was conducted by quality filtering using fastQC. We followed the Genome Analysis Toolkit (GATK) best practices workflow for improving the quality of variant calls. Sequencing reads in the targeted region were aligned and compared to the human reference genome (UCSC hg19) using BWA-MEM version 0.7.10 and Picard tools version 1.119 (http://broadinstitute.github.io/picard/). In the case of CRCs, alignment was performed using the combination of human and mouse reference (UCSC mm10) sequences, to remove false positive variants from mouse contamination through feeder layer. According to the GATK best practice, the location of insertions and deletions was recalibrated based on the dbSNP database, version 150, of known variants. Cross-contamination ratio was estimated using ContEst [18] (Supplementary Fig. 1) to identify cross-contamination between the tumours and CRC samples.

3.5.1. Somatic single-nucleotide variant (SNV) and indel calling

SNVs and indels were identified in normal-tumour pair and normal-CRC pair samples by GATK, version 4.1.2.0 Mutect2 [19]. SNVs in 83 targeted genes were annotated with genetic features using SnpEff version 4.3, to obtain the common somatic mutation list based on the Catalog of Somatic Mutation in Cancer database (COSMIC) for annotated mutations [20,21].

Additionally, we used PROVEN version 1.1.5 and SIFT version 6.2.1 to predict the effects of mutations on biological functions [22,23].

To retain high-confidence somatic variants, we applied the following filtering criteria provided in Mutect2: [1] variants with alternative allele counts less than 5, [2] variants with total allele counts (read depth) less than 20, and [3] variants with allele frequency (AF) less than 0.05. The candidates who fulfulled the above criteria were manually checked using Integrative Genomics Viewer (IGV) version 2.3.81 to evade false-positive variants (Supplementary Fig. 2) [24]. The mutations detected in both, tumour and paired CRCs of the same patient were defined as concordance mutations. The concordance rate was calculated as the formula below for primary-CRC pairs

$$concordance\ rate\ =\ \frac{count\ of\ shared\ mutations}{count\ of\ total\ mutations}$$

While primary-only mutation was detected as a somatic mutation in primary tumours, the mutation failed to pass the filtering criteria in the paired CRCs. A mutation is defined as a CRC-only mutation, when it is detected in CRCs as a high-confidence somatic variant, but is not present in the tumour. In order to confirm that a mutation existed in both tumour and matching CRCs, we checked the presence of alternative allele using IGV in the location where the somatic mutation occurs (Supplementary Fig. 2). We checked the tumour and CRCs-only mutations individually using IGV and included them in the concordant mutation category if a low-frequency allele was present in the counterpart.

3.5.2. Copy number variant (CNV) calling

CNV calling was performed using CNVkit version 0.8.6.9 [25]. The corrected on- and off-target log2 values of bin-level copy ratios with associated weights were concatenated using the *fix* command. The *call* command with the center mode option was used to recalculate the copy number of the default center-centering the copy number neutral area slightly above or below the expected log2 value of zero. After these adjustments, we used the threshold method to calculate the absolute integer copy number of each segment.

3.5.3. RNA sequencing and characterization of molecular subtype

RNA sequencing using TruSeq Stranded Total RNA Sample Prep Kit with Ribo-Zero H/M/R was performed to confirm the similarity between the original PDAC tissue and CRCs even at the gene expression level. We trimmed the FASTQ files to obtained clean cropped read with length 100 using Trimmomatic [26]. In the case of CRCs, the FASTQ files used Disambiguate removed mouse contamination through feeder layer [27]. STAR and Cufflinks are mapped the read to transcriptome as a reference and calculated normalized gene-level expression values such as FPKM (Fragments Per Kilobase Million) [28,29]. The analysis of the molecular subtype of CRCs and original tissue proceeded in the same way as described in the previous paper in 2017 [30,31]. We divided the samples into two groups, known as Moffitt subtypes, based on 50 genes expression. Based on 62 genes expression, we also identified three groups known as Collisson subtypes (classical, quasi-mesenchymal, and exocrine).

3.6. Establishment of patient-derived xenografts (PDX) using CRCs

Exponentially growing PDAC CRCs were trypsinized, dispersed into single cells, and suspended in 200 μL of Matrigel HC (BD Biosciences). To evaluate tumourigenicity *in vivo*, 2×10^6 cells prepared in 0.2 mL of Matrigel were injected subcutaneously into the flank region of 5-week-old male NOD/SCID mice with severe combined immunodeficiency (National Cancer Institute, USA). The mice were sacrificed by CO2 inhalation; tumours were harvested once they reached a volume of approximately ~1500 mm3 (20 mm). PDX tumour tissue was divided for: 1) fixation in 10% buffered formalin for paraffin embedding/histology, 2) cryopreservation, 3) PDX cell line development and passaging, and 4) optimal cutting temperature compound embedding. Inclusion criteria are 5-week-old, male, and NOD/SCID mice) and exclusion criteria is that animal might be dropped from the study and euthanized before the predetermined time point if the size of a subcutaneous tumour exceeds 20mm. The primary outcome measure that was used to determine the sample size was the diameter and volume of tumour mass. In order to evaluate the response to chemotherapeutic agents in xenograft models from the CRCs, we performed the randomization of 12 mice into two groups (treatment group, n=6; control group, n=6). We injected gemcitabine in chemotherapeutic group (Gemcitabine, 50 mg/kg, twice/week). Animals were housed at the Yonsei University animal care facility in accordance with the institutional guidelines. All experiments were performed in accordance with the relevant animal use guidelines.

3.7. Cell viability assay and drug sensitivity

The cell viability assay was performed to determine the drug sensitivity of each cell line. CRCs of patients with different prognoses were selected to test the response to anticancer agents. The responder group was defined as follows: [1] patients who had complete remission (CR)/partial response (PR)/ stable disease for at least 4 months or [2] patients who had CR or PR at best. Cells were seeded in 96-well plates at a density of 5,000 cells per well. To identify compounds that are toxic to CRCs, after attachment, the cells were exposed to gemcitabine, 5-FU, oxaliplatin, irinotecan, nab-paclitaxel, and combinations of these drugs for 72 h. CellTox Green (Promega, Heidelberg, Germany) was added to the growth medium in accordance with the manufacturer's instructions, and the cells were followed by live cell imaging using the IncuCyte microscope (Essen Bioscience) to identify toxicity. The data from the images were

quantified using the IncuCyte software (version 2011A rev2) and the data plots of cell toxicity extraction and proliferation were plotted using the GraphPad Prism software. Values are the means of triplicate wells from three independent experiments for each drug concentration.

3.8. Key resource table

Reagent or resource	Source	Identifier
Antibodies		
Rabbit polyclonal anti-a-Amylase	Santa Cruz Biotechnology	Cat# SC−25562, RRID:AB_633872
Mouse monoclonal anti-Cytokeratin19	Santa Cruz Biotechnology	Cat# SC-6278, RRID:AB_627851
Mouse monoclonal anti-Insulin	Santa Cruz Biotechnology	Cat# SC-8033, RRID:AB_627285
Mouse monoclonal anti-Vimentin	Cell signaling technology	Cat# 5741, RRID:AB_10695459
Mouse monoclonal anti-S100A2	Sigma-Aldrich	Cat# S6797, RRID:AB_261539
Goat polyclonal anti-GATA6	R and D Systems	Cat# AF1700, RRID:AB_2108901
Alexa Fluor 594	Thermo fisher scientific	Cat# A27016, RRID:AB_2536080
Alexa Fluor 488	Thermo fisher scientific	Cat# A28175, RRID:AB_2536161
DAPI	Vector Laboratories	Cat# H-1200, RRID:AB_2336790
Oligonucleotides		
PCR primers for KRAS		
Forward primer: AGGCCTGCTGAAAATGACTGA	Bioneer corp.	N/A
Reverse primer: GGTCCTGCACCAGTAATATGCA	Bioneer corp.	N/A
Chemicals and recombinant protein		
Y-27632 dihydrochloride	Enzo Life Science	Cat# ALX-270-333
Nutrient mixture F-12 HAM'S	hyclone	Cat# SH30026.01
DMEM/high glucose	hyclone	Cat# SH30243.01
Hydrocortisone	Sigma	Cat# H-0135
Human Epitherial growth factor	Gibco	Cat# PHG0313
Insulin	Sigma	Cat# I-9278
AmphotericinB	Thermo fisher scientific	Cat# A2942
Gentamycin	GIBCO	Cat# 15750-060
Cholera toxin	Sigma	Cat# C-8052
Adenine	sigma	Cat# A2786
Agar	Thermo fisher scientific	Cat# BD214220
Collagenase I	Gibco	Cat# 17100-017
Collagenase IV	Gibco	Cat# 17104-019
QIAamp DNA Mini kit	Qiagen	Cat# 51304
RNeasy Mini kit	Qiagen	Cat# 74104
Alcian blue stain kit	Vector laboratories	Cat# H-3501
Matrigel	BD Biosciences	Cat# 356234
zylene	Ducsan	Cat# H29118
Ethanol	Millipore corp.	Cat# 100983
Methanol	Millipore corp.	Cat# 106012
Hydrogen peroxidase	FUJIFILM	Cat# 081-04215
TritonX-100	Sigma	Cat# T8787
Citrate tribasic dihydrate	Sigma	Cat# S4641
Horse serum	Thermo fisher scientific	Cat# 16050130
Fetal bovine serum	Thermo fisher scientific	Cat# 16000-044
ReliaPrep FFPE gDNA Miniprep system	Promega	Cat# A2352
Thiazolyl Blue Tetrazolium Bromide	Sigma	Cat# M2128
Gemcitabine	Lilly	Cat# 7502
Cell lines		
YPAC-2	Severance Hospital, Seoul, Korea	N/A
YPAC-5	Severance Hospital, Seoul, Korea	N/A
YPAC-6	Severance Hospital, Seoul, Korea	N/A
YPAC-7	Severance Hospital, Seoul, Korea	N/A
YPAC-10	Severance Hospital, Seoul, Korea	N/A
YPAC-13	Severance Hospital, Seoul, Korea	N/A
YPAC-15	Severance Hospital, Seoul, Korea	N/A
YPAC-16	Severance Hospital, Seoul, Korea	N/A
YPAC-17	Severance Hospital, Seoul, Korea	N/A
YPAC-20	Severance Hospital, Seoul, Korea	N/A
YPAC-21	Severance Hospital, Seoul, Korea	N/A
YPAC-23	Severance Hospital, Seoul, Korea	N/A
YPAC-25	Severance Hospital, Seoul, Korea	N/A
YPAC-26	Severance Hospital, Seoul, Korea	N/A
YPAC-27	Severance Hospital, Seoul, Korea	N/A
YPAC-28	Severance Hospital, Seoul, Korea	N/A
YPAC-29	Severance Hospital, Seoul, Korea	N/A
YPAC-30	Severance Hospital, Seoul, Korea	N/A
YPAC-31	Severance Hospital, Seoul, Korea	N/A
YPAC-32	Severance Hospital, Seoul, Korea	N/A
YPAC-33	Severance Hospital, Seoul, Korea	N/A
YPAC-34	Severance Hospital, Seoul, Korea	N/A
YPAC-35	Severance Hospital, Seoul, Korea	N/A
YPAC-37	Severance Hospital, Seoul, Korea	N/A

(*continued*)

YPAC-39	Severance Hospital, Seoul, Korea	N/A
YPAC-43	Severance Hospital, Seoul, Korea	N/A
YPAC-44	Severance Hospital, Seoul, Korea	N/A
YPAC-46	Severance Hospital, Seoul, Korea	N/A
Swiss 3T3-J2 cell(fibroblast, mouse)	Geogetown University	N/A
Experimental Models: strains		
NOD/SCID	National Cancer Institute.USA	N/A
BALB/c Nude	Institute of Medical Science,University of Tokyo	N/A

3.9. Statistical analysis

All statistical analyses were performed using GraphPad Prism 7 software. IC 50 value were statistically analysed using Student's t test, and the graphs show the mean ± SD. Differences between groups were considered to be significant at a P value of <0.05. We did not include additional statistical tests for data distributions.

3.10. Role of funders

This research was supported by the Basic Science Research Program through the National Research Foundation of Korea (NRF) funded by the Ministry of Science, ICT & Future Planning (Grant No.: 2014R1A1A1006272). This research was supported by a grant of the Korea Health Technology R&D Project through the Korea Health Industry Development Institute (KHIDI), Funded by the Ministry of Health & Welfare, Republic of Korea (grant number: HI19C0642-060019). This work was supported by the National Research Foundation of Korea (NRF) grant funded by the Korea government (MSIT) (No. 2019R1A2C2008050). This work was supported by the National Research Foundation of Korea (NRF) grant funded by the Korea government (2020R1A2C209958611 and 2020M3E5E204028211). The funders did not have any role in the study design, data acquisition, analysis, interpretation, writing, or submission of the manuscript.

4. Results

4.1. Establishment of CRCs from clinical specimens

We established a total of 28 CRCs from patients who were pathologically diagnosed with PDAC. The following were the original sources for tissue acquisition: surgical resection (n=12), EUS-guided biopsy (n=15), and percutaneous liver biopsy (n=1) (Supplementary Table 2). Subsequently, we performed genomic analysis of 9 patient samples, in which the original FFPE tissue contained sufficient amount of DNA (>1 μg) after microdissection. Drug screening was performed in 7 patients who showed a defined chemotherapeutic response.

4.2. Characterization of CRCs

Epithelial colonies were readily observed at 2 days and rapidly proliferated to reach confluence in approximately 7-14 days (Fig. 2a). Immunofluorescence for CRCs was performed using a monoclonal antibody against cytokeratin 19. The cytoplasm of cancer cells was clearly stained with this antibody (Fig. 2b and Supplementary Fig. 3) Soft agar colony formation assay showed *in vitro* tumourigenesis (Fig. 2d). All colony assays can be divided into three groups by their growth (large size and rapid growing, moderate, small size and slow growing). YPAC-2, 5, 26, 35, and 46 showed large colony formation and rapid growing feature. In contrast, YPAC-10, 15, 16, 23, 25, 29,

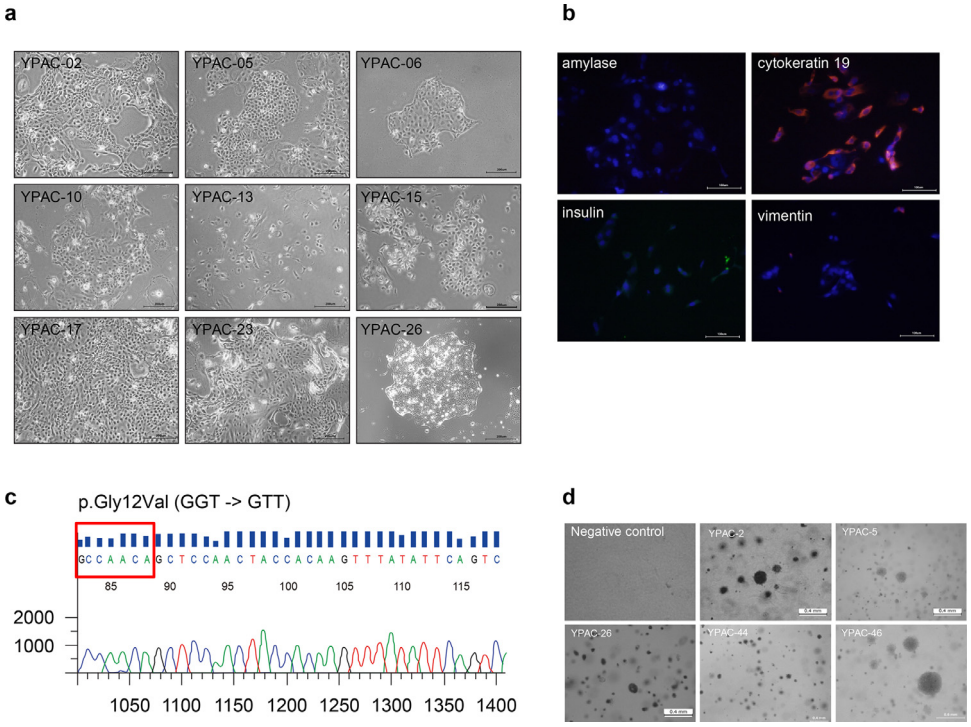

Fig. 2. Characterization of conditionally reprogrammed cell lines (representative image). (a) Conditionally reprogrammed cell formation was confirmed after 15 days of culture, and within one month. (Scale bar, 200 μm) (b) Characterization of the intensely fluorescent cells in conditionally reprogrammed cells. (Scale bar, 100 μm) (c) *KRAS* mutations were analysed by polymerase chain reaction (p.Gly12Val (GGT → GTT)). (d) Soft agar colony formation assay showed *in vitro* tumourigenesis.

30, and 34 showed small colony formation and slow growing feature. Large colony group showed relatively larger tumour size at their diagnosis, many proportion of unresectable cancer stage, metastatic status. CRCs with aggressive cancer characteristics showed large colony formation and rapid growth (Supplementary Fig. 4 and Supplementary Table 6). With respect to the key oncogenic mutations, PCR was used to perform *KRAS* mutation (Fig. 2c and Supplementary Fig. 5). Of the 28 samples, 27 showed *KRAS* mutations in codon 12/13 (n=25, *KRAS* mutation was confirmed by targeted sequencing. Sanger sequencing was not performed for 1 patient sample because of low amount of DNA) or codon 61 (n=1).

4.3. Genetic characterization of patient-derived models

4.3.1. Sample pair matching

To verify the origin of the patient-derived models, all the 9 CRCs and their matched primary tissues used in this study were checked for their germline single-nucleotide polymorphism (SNP) similarity (Fig. 3a). CRCs were matched with their paired blood and original tumour tissue. In addition, the proportion of exonic variations was well retained among the primary pancreatic cancer tissues and the corresponding cancer CRCs (Fig. 3b). Analysis of the distribution of base substitutions in both pancreatic cancer tissues and CRCs revealed over-representation of C>T transition; this is in agreement with the mutational spectrum presented in previous studies [32].

4.3.2. Genetic variants

In the initial call, 36 somatic mutations were detected from each set of the 9 primary tumours and 9 CRCs. We found that 30 of these mutations were shared in the primary-CRC pairs (Fig. 4a, Supplementary Table 3 and 4), leaving two primary-only, and four CRC-only mutations. The shared mutations included key oncogenic mutations such as *KRAS* (9 pairs), *TP53* (8 pairs), and *SMAD4* (3 pairs). The overall number of non-synonymous mutations per patient was consistent with that presented in a previous report (median of 2 SNVs, 4.27 per Mb) [33]. The two primary-only mutations were, a synonymous mutation in *ATRX* (YPAC-2) and an intron variant in *NPM1* (YPAC-17), implying a low phenotypic impact. Furthermore, deeper assessments identified that the four CRC-only mutations were not de novo but had pre-existed in alleles from matching primary tumours at low AF, which only became callable with an increase in VAFs (see Methods, Supplementary Fig. 2). While primary tumour specimens normally contain non-tumourous cells (e.g., stromal cells), frequently in high numbers (e.g., 30-80%), increased tumour cell purity in CRCs enables more accurate profiling of somatic mutations [34]. Overall, the 9 CRCs preserved the genetic characteristics of the primary tumours with high concordance, with additional confirmation of low-AF *NPM1* mutation in CRC (35 shared mutations out of total 36, concordance rate=97.2%).

The presented AFs of the 36 shared mutations confirmed the clarity of genomic profiles in the CRCs (Fig. 4B). The list of genes with mutations was preserved and the overall VAFs were increased in

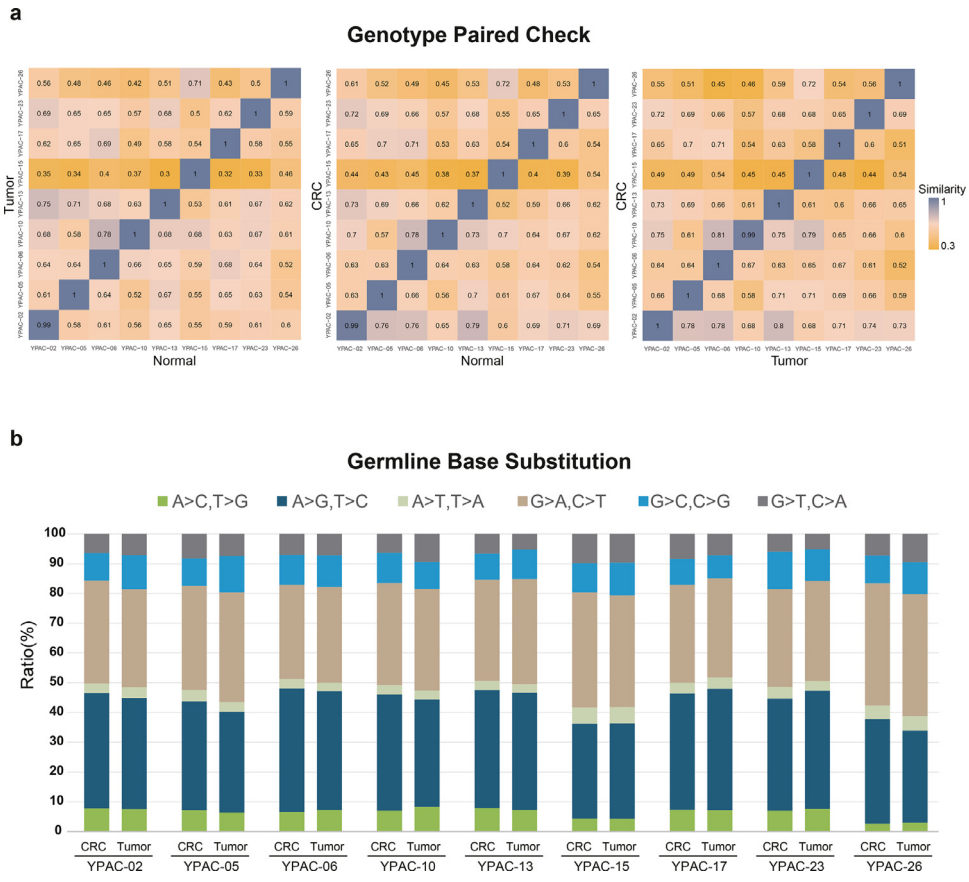

Fig. 3. Sample pair matching. (a) The concordance ratio of germline single-nucleotide polymorphisms (SNPs) of objects on the y-axis to the x-axis is defined as the similarity score and the closer the maximum value is to 1, higher is the similarity, represented by blue colors. Nine conditionally reprogrammed cell lines (CRCs) were matched with their paired blood (normal) and original tumour tissue. Furthermore, we confirmed the genetic coincidence and originality between the original tissue and patient-derived model. Colors indicate the similarity of paired samples, with high similarity represented by blue and low similarity represented by yellow. (b) The proportion of base substitutions was maintained in a similar pattern in each of the primary pancreatic cancer tissue and corresponding cancer CRCs, confirming that they were from the same individual. (For interpretation of the references to color in the text, the reader is referred to the web version of this article.)

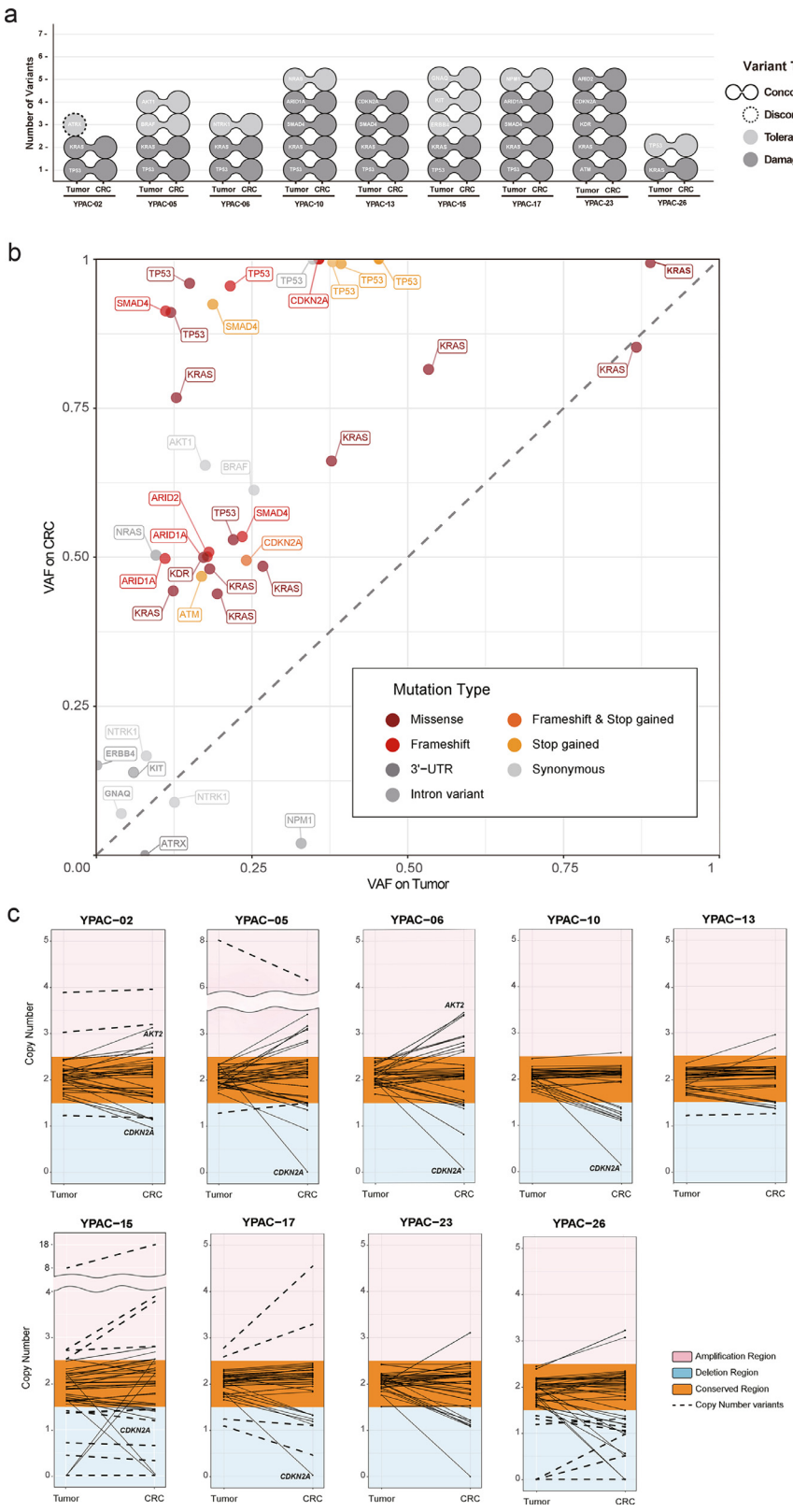

Fig. 4. Genetic characterization. (a) The two connected circles indicate the somatic mutation detected in both the primary and the CRC, and the single circle implies that the expressed mutation was detected only in either the primary or the CRC. The effects on biological functions due to allele change were distinguished by color, wherein light grey color represents the tolerant effect of the mutation such as synonymous mutation and intron variants. The dark grey color indicates the damaging effect of the mutation such as missense variant and frameshift. The nine CRCs represent the concordance of somatic mutation with the exception of the tolerant mutation of YPAC-2 marked as the dashed line. (b) The x-axis represents the variant allele frequency (VAF) of the mutations in the primary tissue; the y-axis represents the VAF of the mutations in the CRC. In addition, the allele frequency plot shows the gene name and mutation type for each mutation, which are color-coded, and tolerant mutations are marked in grey. (c) The graph indicates comparison between the copy number in the primary tumour (left on the x-axis) and CRCs (right on the x-axis) for 83 targeted genes. The copy number on the y-axis with a value 2.5 or higher is marked as amplification, colored with red and deletion as blue for 1.5 or less of copy number. The unaltered copy numbers in the primary tumour and CRCs are marked as conserved and represent the orange area. Copy number variants (CNVs) are marked with bold dotted lines. (For interpretation of the references to color in the text, the reader is referred to the web version of this article.)

CRCs (average VAF=60.9%) compared to those in primary tumours (24.5%). Specifically, in *KRAS* mutations (i.e., confident drivers and expected to be clonal in all tumour cells), the VAFs were less than 30% in 5 out of 9 primary tumours (12.3-26.7%), which strongly suggests low tumour purity in the specimen. In the matching CRCs, the VAFs were increased to approximately 50% (Fig. 4B). Similar or a significant increase of VAFs was also observed in other key mutations including *TP53* (25.9% to 89.1%), *SMAD4* (17.7% to 79.1%), *CDKN2A* (29.9% to 74.8%), and *ARID1A* (14.4% to 50%). We noted that the VAFs of some mutations (e.g., *TP53*) reached approximately 100%, which can be obtained either by homozygous mutation, loss of heterozygosity (e.g., loss of wild-type copy), or multi-copy amplification. While many studies have observed these copy number changes during tumour progression [35], there could also be a possibility for selective advantage during the generation of CRCs, which requires further investigation to separate these effects.

Likewise, all the 27 CNVs (18 deletions and 9 amplifications) initially called in primary tumours were retained in CRCs (Fig. 4C, Supplementary Table 5). Moreover, the estimated copy numbers (CNs) of the 83 targeted genes remained comparable in CRCs (average CN of 2.00 vs. 2.00). Of note, we found that the degree of copy number changes in key oncogenic CNVs including *CDKN2A* deletion (1.9 vs. 0.6) and *AKT2* amplification (1.9 vs. 2.2) was increased in CRCs. The increased somatic mutation VAFs suggest that CNVs can be better clarified by constructing CRCs.

On WES, The mutation burden of 173 TCGA-PAAD samples was distributed from 1 to 115 (average 37.03). Comparing to TCGA mutation burden, we found that the mutation burden in 10 CRC samples was distributed from 44 to 111 (average 48.43), the same as in previous reports (Supplementary Fig. 6). CRCs were matched with their paired blood and original tumour tissue for their germline SNP similarity (Supplementary Fig. 7). As a result of the WES analysis, 100% (10/10) of the total samples have *KRAS* mutations and 60% (6/10) of the total samples have *TP53* mutations, the key gene of Pancreatic Adenocarcinoma, as shown in the TCGA-PAAD analysis (Supplementary Fig. 8).

4.3.3. Molecular subtype

We confirmed the preservation of subtypes between CRCs and their corresponding primary tumours by using four primary-CRCs pairs (YPAC-5, 17, 23, 26) (Fig. 5). All samples showed a concordance between subtype based on mofitt et al. and half of samples maintained their molecular subtype based on collison et al(30, 31). YPAC-5, 26 were classified as basal type and YPAC-17, 23 were classified as classical type through transcriptome analysis. In transcriptome analysis, key gene expression such as *GATA6, HNF4A* of classical type was higher in YPAC 17, 23 (Fig. 5a). To validate the critical gene expression, we investigated the immunofluorescence expression of *GATA6* and *S100A2* between original tissue slide and CRCs (Fig. 5b). *S100A2* and *GATA6* expression in tumour tissue was consistent with the expression of matched CRCs for YPAC-23 and 26. Classical type YPAC-23 and its original tumour tissue simultaneously showed low signal intensity of S100A2 and high signal intensity of GATA6. Compared to YPAC-23, basal type YPAC-26 and its original tumour tissue simultaneously showed high signal intensity of S100A2 and low signal intensity of GATA6.

4.3.4. In vivo tumourigenesis

In vivo, three CRCs (YPAC-2, 5, 21) were implanted in three NOD/SCID mice, respectively (Supplementary Fig. 9). Implanted CRCs showed tumour engraftment and the grafted tumours were palpated in the flank of mice after 2-3 months (Fig. 6a, YPAC-2). YPAC-21 was from a patient with cystic adenocarcinoma tumour tissue. Mouse xenografted tumours were also mucinous (Fig. 6b and Supplementary Fig. 10), similar to the original tumour phenotype. Histological analysis showed the presence of atypical cells. They were distributed in mucin-filled cysts lined by stacked layers of dysplastic epithelial cells with high nucleus-to-cytoplasm ratio. Hematoxylin and eosin staining showed that the implanted tumour tissues shared similar morphological features with the parent tumour tissue (Fig. 6c). After targeted deep sequencing and sanger sequencing, we confirmed the *KRAS* mutation type was matched with original tumour (YPAC-2, 5) (Supplementary Fig. 11). In order to evaluate the response to chemotherapeutic agents in xenograft models from the CRCs, we implanted

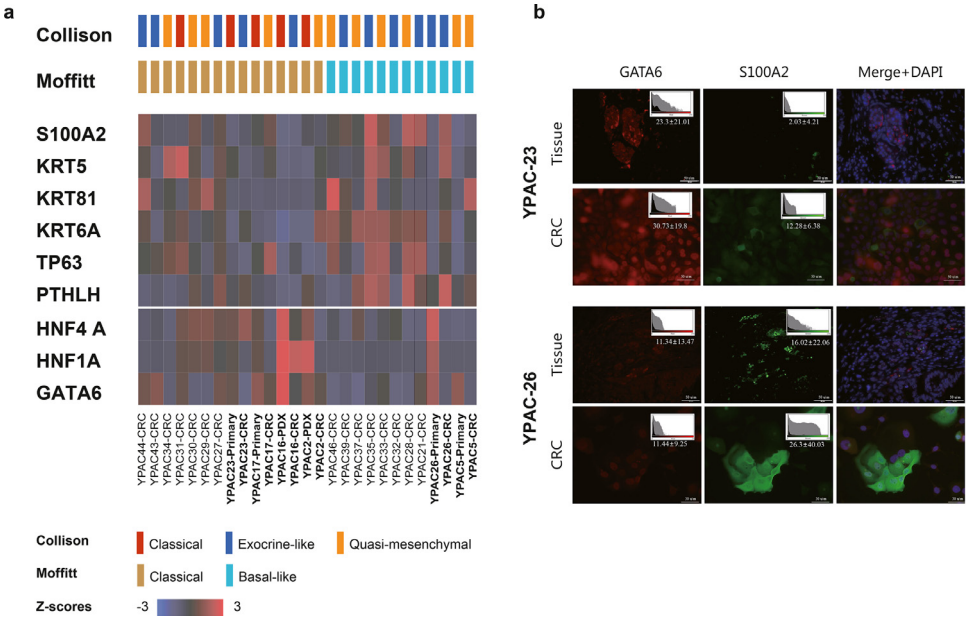

Fig. 5. Preservation of molecular subtypes between CRCs and their corresponding primary tumours (YPAC-5, 17, 23, 26). (a) YPAC-5, 26 were classified as basal type and YPAC-17, 23 were classified as classical type through transcriptome analysis. In transcriptome analysis, key gene expression such as *GATA6, HNF4A* of classical type was higher in YPAC 17, 23. (b) Immunofluorescence expression of *GATA6* and *S100A2* between original tissue slide and CRCs. Classical type YPAC-23 and its original tumour tissue simultaneously showed low signal intensity of S100A2 and high signal intensity of GATA6. Compared to YPAC-23, basal type YPAC-26 and its original tumour tissue simultaneously showed high signal intensity of S100A2 and low signal intensity of GATA6. (Scale bar, 50 μm)

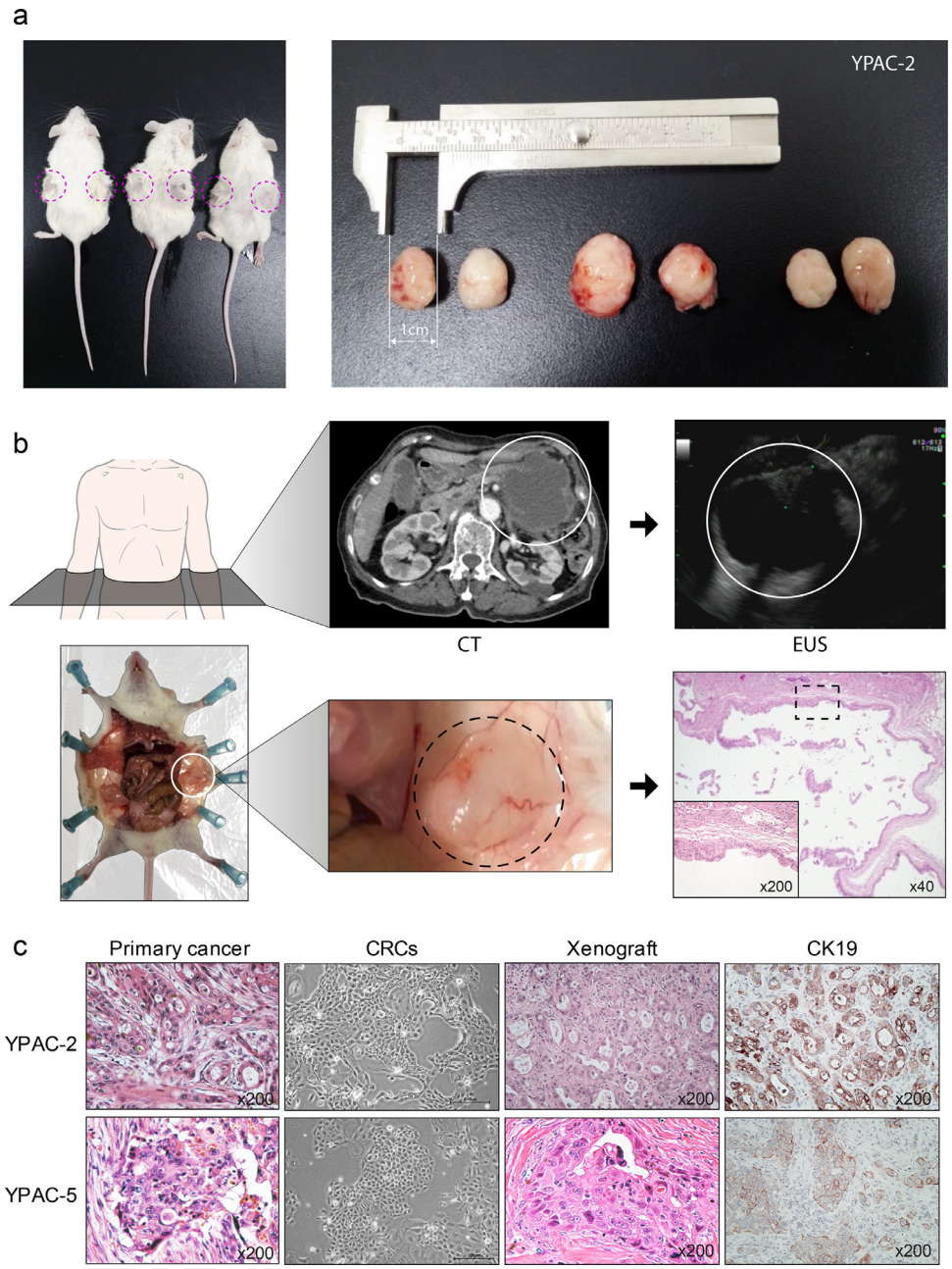

Fig. 6. *In vivo* tumourigenesis. (a) Implanted CRCs (YPAC-2) showed successful tumour engraftment, and a 15 mm sized transplanted tumour on the side of the mouse was palpated after three months. (N=3, Supplementary Fig. 9) (b) CRCs of a patient who was diagnosed with cystic adenocarcinoma showed similar phenotype in mouse CRC implantation. White circle, cystic adenocarcinoma; Black dotted circle, implanted cystic tumour; black dotted square, mucin-filled cysts lined by layers of dysplastic epithelial cells (c) Histological examination showed that CRCs and xenograft were phenotypically similar when compared with primary cancer tissue. CK19, cytokeratin 19. (Scale bar, 200 μm)

the pancreatic cancer patient-derived CRCs in the flank of mouse (vehicle, n=6; gemcitabine, n=6). And, we injected normal saline in vehicle group and gemcitabine in chemotherapeutic group. We found the anti-tumour effect of gemcitabine using xenograft model derived from the CRCs (Supplementary Fig. 12).

4.4. Drug sensitivity assay

We compared responses to anticancer agents in CRCs, with the clinical response of pancreatic cancer patients. Therapeutic options for pancreatic cancer patients include combination chemotherapy regimens with gemcitabine/nab-paclitaxel or FOLFIRINOX (5-fluorouracil, leucovorin, irinotecan, and oxaliplatin). Based on responsiveness to chemotherapy, we divided the patients into a responder group (YPAC-25, 26, 30) and non-responder group (YPAC-2, 5, 16, 31). Other patients showed intermediate responsiveness, therefore we did not perform drug sensitivity test. Results of the cell viability assay indicated that the anti-proliferative effect of anticancer agent was significantly higher in YPAC-25, 26, 30 than in YPAC-2, 5, 16, 31. Drug sensitivity of CRCs corresponded with individual patient's anticancer treatment response. CRCs of the responder group were more sensitive to anticancer agents than those of the non-responder group (Fig. 7a-e). The IC50 value of each drug was statistically lower in the responder group than in the non-responder group (Fig. 7f and g). In a clinical setting, YPAC-2 patient showed increased tumour size in the first chemotherapy response just after 2 months. However, YPAC-25 patient showed good response with decreased tumour size for over 12 months compared to YPAC-2 patient (progression free survival,

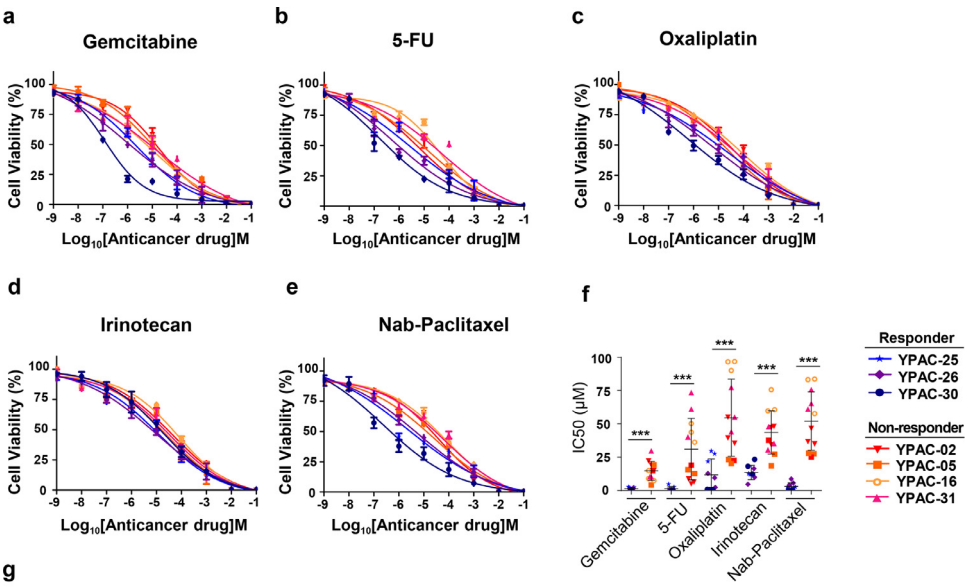

g

Drug	Parameter	Responder			Non-responder			
		YPAC-25	YPAC-26	YPAC-30	YPAC-02	YPAC-05	YPAC-16	YPAC-31
Gemcitabine	IC50 (μM)	2.315	0.9581	0.1239	18.58	10.58	10.03	15.30
	AUC	0.418	0.410	0.337	0.488	0.492	0.448	0.464
	Std.error	±6.05	±0.58	±0.17	±7.48	±9.37	±5.32	±7.17
5-FU	IC50 (μM)	2.616	0.5844	0.1714	6.46	15.51	44.01	55.59
	AUC	0.435	0.407	0.372	0.458	0.466	0.492	0.497
	Std.error	±8.03	±6.31	±7.44	±5.54	±5.5	±4.78	±4.59
Oxaliplatin	IC50 (μM)	26.17	6.10	0.69	42.28	21.51	93.51	52.28
	AUC	0.468	0.458	0.415	0.513	0.499	0.522	0.499
	Std.error	±3.06	±8.99	±5.12	±4.08	±6.96	±3.36	±5.26
Irinotecan	IC50 (μM)	12.15	8.67	18.1	43.01	25.38	65.30	37.11
	AUC	0.469	0.466	0.498	0.520	0.491	0.535	0.499
	Std.error	±5.43	±7.55	±8.66	±5.18	±8.02	±4.74	±4.21
Nab-Paclitaxel	IC50 (μM)	2.31	5.81	0.23	39.33	26.82	74.46	67.19
	AUC	0.449	0.455	0.384	0.488	0.478	0.511	0.503
	Std.error	±4.30	±4.13	±2.88	±2.77	±2.44	±3.82	±3.71

Fig. 7. Conditionally reprogrammed cell lines reveal heterogeneity of chemotherapeutic response. The results of the cell viability assay indicated that the anti-proliferative effect of the anticancer agent was significantly higher in YPAC-25, 26, and 30 than in YPAC-2, 5, 16 and 31. Drug sensitivity of CRCs correlated with individual patient anticancer treatment response. CRCs of responder group were more sensitive to anticancer agents than those of the non-responder group. Viability assay were performed at least two times in triplicate experiments. ***, $P < 0.0001$. AUC, Area Under The Curve [IC50 value was statistically analysed using Student's t test, and the graphs show the mean ± standard deviation]

360 vs. 65 days) (Supplementary Fig. 13). *Ex-vivo* examination of patient-derived cell lines also showed similar drug responsiveness, which matched with clinical results.

5. Discussion

We established cell culture models derived from tumour samples of PDAC patients and then performed genetic analyses using these cells. The key oncogenic mutation present in the tumour tissue was reliably identified in the derived cell line. CRCs can be isolated from patients at all stages of pancreatic cancer using the limited tissue available from a fine needle tumour biopsy as the starting tissue.

To date, various cancer models have been developed for cancer research. At first, cancer cell lines also exhibit tumour characteristics but long-term culture is difficult and individual patient-derived matched model is difficult to develop. A few models have been developed using primary PDAC to establish stable cancer cell lines [36-38], and varying success rates (7.4-74.1%) have been reported [39,40]. However, commercialized cancer cell line models have repeatedly shown technical and biological limitations including cellular senescence, reduced stability over time, and insufficient recapitulation of the primary tumour [7,9,41,42]. Moreover, generating patient-derived xenograft models (PDX) commonly used for cancer research requires a cost- and time-intensive endeavor (more than 4-6 months). Though the recently developed 3D cancer model, called organoid, recapitulates the original tumour, it stimulates LGR5 (+) stem-like cells during the formation of initial tumours [41]. Recently, studies have reported that for organoid culture—although the culture needs many niche factors—the composition of the surrounding niche factors still changes in pancreatic cancer [41,43,44]. Above all, niche factors can also affect the result of drug screening through chemical reaction and, considerable financial resources are required for high-throughput drug screening using the organoid culture [8].

In previous studies, the success rate of CRC culture was found to differ according to cancer type (from 24.2 to 50%) [10,45–47]. For pancreatic cancer, Liu et al. developed four cell lines (2 tumour and 2 normal) from 8 pancreatic tissue samples [10]. Natalya et al. reported three cell line models from surgical tissue for pancreatic cancer, but the number of patients was too small to characterize the method [46]. The present study was the largest to develop PDAC CRCs. Further, previous studies have been conducted using surgical tissues that account for only 10% to 20% of PDAC. In this study, we performed experiments using endoscopic biopsies of patients with inoperable PDAC who are large proportion of PDAC, indicating the novelty of this study. Histology-based morphological analysis revealed similarities between mutations in matched samples, primary tumours, and CRCs, with increased AF observed in CRCs. *KRAS, TP53*, and *SMAD4* are representative somatic mutations of pancreatic cancer [48]. In samples subjected to sequencing and PCR, these typical mutations were detected. Furthermore, the key oncogenic mutations—present at a low AF in the tumour—showed an increased AF in CRCs. This may

be a useful tool for detecting minor allele deficiency mutations in cancer.

Even if the CRC protocol is obviously less lab-intensive and more affordable, tumour organoid culture is well-established method for in vitro maintenance of patient-derived samples. For side-by-side comparison to the success rate in both methods, previous studies for CRCs showed 50~100% success rate, even if the number of sample was small (3~5 cases) and there was no enough information about the tissue acquisition route [10,46,49]. In case of organoids, the success rate of between 66% and 100% for samples from fine needle biopsy is reported by previous researchers [44,50,51]. But, there have been no large-scale studies of fine needle biopsy in CRCs. Second, there are few studies to investigate molecular feature of CRC methods in PDAC rather than organoid culture, previously. In other cancer type, they showed the maintenance of molecular feature in CRC matched with original tumour and preserved key mutation and tissue heterogeneity [52]. Beglyarova et al. demonstrated the MYC−ERCC3 interaction as a target for PDAC and a new mechanistic approach for the disruption of critical signaling in MYC-dependent cancers using the patient-derived pancreatic cancer CRCs [46]. Relatively, several studies reported the preservation of similar molecular characteristics in organoids compared to matched cancer tissue [44,51]. Tuveson et al. found that pancreatic cancer patient-derived organoids therapeutic profiles paralleled patient outcomes. They proposed that combined molecular and therapeutic profiling of organoids may predict clinical response and enable prospective therapeutic selection [44].

Precision medicine focuses on delivering the most appropriate therapy to a patient through drug screening based on the clinical and molecular features of their disease. In the present study, CRCs showed similar characteristics to those of the original tumour samples. We tested the feasibility of using CRCs derived from metastatic pancreatic cancers as drug screening tools and validated the robustness of our approach. The drug sensitivity test revealed that anti-cancer drug sensitivity was reliably associated with patient prognosis. By evaluating the drug sensitivity of a large panel of clinical agents using CRCs, this platform might identify a targetable new drug [46].

Recent developments in genomic medicine for PDAC treatment have provided various options for personalized treatment [30,31,53−58]. Studies have been reported wherein patients were divided into several groups based on their responsiveness to chemotherapy and survival [53-56,59−61]. In PDAC research, major limitations in implementing treatment strategies based on mutational status are the availability of tumour samples for detailed sequence analysis., In addition, [1] difficulty in primary cell culture owing to limited life span, [2] difficulty in tumour sequencing owing to the dominance of stromal cells, and [3] absence of an appropriate preclinical model preserving the molecular characteristics of tumour cells are also serious limitations. Therefore, generating CRCs for amplifying tumour epithelial cells could serve as an important preclinical strategy. Established CRCs of pancreatic cancer predominantly comprising neoplastic cells thereby enable scientists to study low frequency nucleotide variants and copy number alterations that would be difficult to discern in primary tumour tissue with low neoplastic cellularity. Furthermore, most primary cell cultures are difficult to maintain because they have a limited lifespan due to their gradual decrease in proliferation, eventually leading to senescence. In the present study, we maintained YPAC-2 for over 2 years. Therefore, the CRC methodology has wide application potential and can be adapted for live bio-banking and basic research, as well as for diagnostic and therapeutic purposes.

There are several limitations of CRC methodology compared with PDX or organoids. Compared with PDX, some CRC cells derived from malignant tumours were often non-malignant, without tumour-derived mutations. It is also a kind of issue in organoids with normal epithelial cell contamination [62,63]. Researchers try to reduce of normal like organoid using specialized method such as media selection, picking method according to morphology in organoids [64]. In this study, we used refined method as follows: IF such as pancreatic cancer marker, PCR by most common gene *KRAS*, tumour formation assay, and targeted sequencing. Another limitation of CRC is that it cannot recapitulate with tumour microenvironment. It is difficult to evaluate the impact of stromal cells on tumour-cell growth and their effect on the tumour-cell response to treatments. Regarding organoids, recent research for co-culture system with cancer associated fibroblast and/or immune cell is promising [65-68]. Recent study reported organoid culture after CRC establishment which can be a solution of above problem in cancer research [52].

Nonetheless, there are several strengths in CRCs methods. At first, rapid expansion is possible for high throughput drug screening because of the characterization of 2D culture. Additionally, these cultures are more suitable for high throughput rather than low-throughput drug screening. Overall it takes 4-6 weeks to provide enough cells for drug screening. CRC can be reproduced for long periods of time without genomic alterations. Conditionally reprogrammed cells retain cell lineage commitment and maintain the heterogeneity of cells present in a biopsy. Compared to organoids, it does not depend on the extracellular matrix matrigel, which can hamper drug penetration and be adverse in drug screens.

In conclusion, using the conditional reprogramming cell culture technique, we established patient-specific preclinical cancer cell lines. Sequencing analysis revealed that the CRCs maintained the mutations present in the original tumour tissue. The use of matched patient-derived cells provided a unique *ex vivo* model for personalized cancer therapy of PDAC.

6. Author's Contributions

H.S.L., E.K., S.K., and S.B. designed the study and directed the entire study. E.K. and S.K. performed analyses of sequencing data. H.S.L., J.L., C.H.P., S.J.P., and J.M.H. performed in vitro experiments. H.S.L. and S.J. performed statistical analyses. H.K.H., C.M.K., H.K., J.H.J., I.R.C., M.J.C., J.Y.P., S.W.P., S.Y.S., provided samples and clinical data. H.S.L. and E.K. wrote the manuscript. H.K.H., C.M.K., H.K., J.H.J., I.R.C., M.J.C., J.Y.P., S. W.P., S.Y.S. critically reviewed the manuscript. All authors reviewed and approved the final manuscript.

7. Data sharing

Data presented in this study can be downloaded through the Sequence Read Archive (SRA) under BioProject ID: PRJNA673595. The authors declare that all data supporting the findings of this study are available with its supplementary information files. Extra data is available from the corresponding authors upon request. The data can be available to others in de-identified form after all primary and secondary endpoints have been published and in the presence of a data transfer agreement.

Declaration of Competing Interest

The authors declare no conflict of interest.

Acknowledgements

The authors sincerely appreciate all patients who consented to participate in this study. The authors are deeply grateful to Dong-Su Jang, MFA, (Medical Illustrator, Medical Research Support Section, Yonsei University College of Medicine, Seoul, Korea) for his medical illustrations.

Supplementary materials

Supplementary material associated with this article can be found, in the online version, at doi:10.1016/j.ebiom.2021.103218.

References

[1] Rahib L, Smith BD, Aizenberg R, Rosenzweig AB, Fleshman JM, Matrisian LM. Projecting cancer incidence and deaths to 2030: the unexpected burden of thyroid, liver, and pancreas cancers in the United States. Cancer Res 2014;74(11):2913–21.
[2] Ryan DP, Hong TS, Bardeesy N. Pancreatic adenocarcinoma. N Engl J Med 2014;371(11):1039–49.
[3] Peters S, Camidge DR, Shaw AT, Gadgeel S, Ahn JS, Kim DW, et al. Alectinib versus crizotinib in untreated ALK-positive non-small-cell lung cancer. N Engl J Med 2017;377(9):829–38.
[4] Soria JC, Ohe Y, Vansteenkiste J, Reungwetwattana T, Chewaskulyong B, Lee KH, et al. Osimertinib in untreated EGFR-mutated advanced non-small-cell lung cancer. N Engl J Med 2018;378(2):113–25.
[5] Vogelstein B, Papadopoulos N, Velculescu VE, Zhou S, Diaz Jr. LA, Kinzler KW. Cancer genome landscapes. Science 2013;339(6127):1546–58.
[6] Ellis MJ, Perou CM. The genomic landscape of breast cancer as a therapeutic roadmap. Cancer Discov 2013;3(1):27–34.
[7] Knudsen ES, Balaji U, Mannakee B, Vail P, Eslinger C, Moxom C, et al. Pancreatic cancer cell lines as patient-derived avatars: genetic characterisation and functional utility. Gut 2017.
[8] Tuveson D, Clevers H. Cancer modeling meets human organoid technology. Science 2019;364(6444):952–5.
[9] Shay JW, Wright WE. Senescence and immortalization: role of telomeres and telomerase. Carcinogenesis 2005;26(5):867–74.
[10] Liu X, Ory V, Chapman S, Yuan H, Albanese C, Kallakury B, et al. ROCK inhibitor and feeder cells induce the conditional reprogramming of epithelial cells. Am J Pathol 2012;180(2):599–607.
[11] Liu X, Krawczyk E, Suprynowicz FA, Palechor-Ceron N, Yuan H, Dakic A, et al. Conditional reprogramming and long-term expansion of normal and tumour cells from human biospecimens. Nat Protoc 2017;12(2):439–51.
[12] Yuan H, Myers S, Wang J, Zhou D, Woo JA, Kallakury B, et al. Use of reprogrammed cells to identify therapy for respiratory papillomatosis. N Engl J Med 2012;367(13):1220–7.
[13] Timofeeva OA, Palechor-Ceron N, Li G, Yuan H, Krawczyk E, Zhong X, et al. Conditionally reprogrammed normal and primary tumour prostate epithelial cells: a novel patient-derived cell model for studies of human prostate cancer. Oncotarget 2017;8(14):22741–58.
[14] Suprynowicz FA, Upadhyay G, Krawczyk E, Kramer SC, Hebert JD, Liu X, et al. Conditionally reprogrammed cells represent a stem-like state of adult epithelial cells. PNAS 2012;109(49):20035–40.
[15] Lee HS, Lee JS, Lee J, Kim EK, Kim H, Chung MJ, et al. Establishment of pancreatic cancer cell lines with endoscopic ultrasound-guided biopsy via conditionally reprogrammed cell culture. Cancer Med 2019;8(7):3339–48.
[16] Palechor-Ceron N, Suprynowicz FA, Upadhyay G, Dakic A, Minas T, Simic V, et al. Radiation induces diffusible feeder cell factor(s) that cooperate with ROCK inhibitor to conditionally reprogram and immortalize epithelial cells. Am J Pathol 2013;183(6):1862–70.
[17] Shin HT, Choi YL, Yun JW, Kim NKD, Kim SY, Jeon HJ, et al. Prevalence and detection of low-allele-fraction variants in clinical cancer samples. Nat Commun 2017;8(1):1377.
[18] Cibulskis K, McKenna A, Fennell T, Banks E, DePristo M, Getz G. ContEst: estimating cross-contamination of human samples in next-generation sequencing data. Bioinformatics 2011;27(18):2601–2.
[19] Cibulskis K, Lawrence MS, Carter SL, Sivachenko A, Jaffe D, Sougnez C, et al. Sensitive detection of somatic point mutations in impure and heterogeneous cancer samples. Nat Biotechnol 2013;31(3):213–9.
[20] Cingolani P, Platts A, Wang le L, Coon M, Nguyen T, Wang L, et al. A program for annotating and predicting the effects of single nucleotide polymorphisms, SnpEff: SNPs in the genome of Drosophila melanogaster strain w1118; iso-2; iso-3. Fly (Austin) 2012;6(2):80–92.
[21] Forbes SA, Bhamra G, Bamford S, Dawson E, Kok C, Clements J, et al. The catalogue of somatic mutations in cancer (COSMIC). Curr Protoc Hum Genet 2008:1. Chapter 10:Unit 10.
[22] Choi Y, Sims GE, Murphy S, Miller JR, Chan AP. Predicting the functional effect of amino acid substitutions and indels. PLoS One 2012;7(10):e46688.
[23] Ng PC, Henikoff SSIFT. Predicting amino acid changes that affect protein function. Nucleic Acids Res 2003;31(13):3812–4.
[24] Robinson JT, Thorvaldsdottir H, Winckler W, Guttman M, Lander ES, Getz G, et al. Integrative genomics viewer. Nat Biotechnol 2011;29(1):24–6.
[25] Talevich E, Shain AH, Botton T, CNVkit Bastian BC. Genome-wide copy number detection and visualization from targeted DNA sequencing. PLoS Comput Biol 2016;12(4):e1004873.
[26] Bolger AM, Lohse M, Usadel B. Trimmomatic: a flexible trimmer for Illumina sequence data. Bioinformatics 2014;30(15):2114–20.
[27] Ahdesmaki MJ, Gray SR, Johnson JH, Lai Z. Disambiguate: an open-source application for disambiguating two species in next generation sequencing data from grafted samples. F1000Res. 2016;5:2741.
[28] Dobin A, Davis CA, Schlesinger F, Drenkow J, Zaleski C, Jha S, et al. STAR: ultrafast universal RNA-seq aligner. Bioinformatics 2013;29(1):15–21.
[29] Trapnell C, Roberts A, Goff L, Pertea G, Kim D, Kelley DR, et al. Differential gene and transcript expression analysis of RNA-seq experiments with TopHat and Cufflinks. Nat Protoc 2012;7(3):562–78.
[30] Collisson EA, Sadanandam A, Olson P, Gibb WJ, Truitt M, Gu S, et al. Subtypes of pancreatic ductal adenocarcinoma and their differing responses to therapy. Nat Med 2011;17(4):500–3.
[31] Moffitt RA, Marayati R, Flate EL, Volmar KE, Loeza SG, Hoadley KA, et al. Virtual microdissection identifies distinct tumour- and stroma-specific subtypes of pancreatic ductal adenocarcinoma. Nat Genet 2015;47(10):1168–78.
[32] Alexandrov LB, Nik-Zainal S, Wedge DC, Aparicio SA, Behjati S, Biankin AV, et al. Signatures of mutational processes in human cancer. Nature 2013;500(7463):415–21.
[33] Lawrence MS, Stojanov P, Polak P, Kryukov GV, Cibulskis K, Sivachenko A, et al. Mutational heterogeneity in cancer and the search for new cancer-associated genes. Nature 2013;499(7457):214–8.
[34] Dennison JB, Shahmoradgoli M, Liu W, Ju Z, Meric-Bernstam F, Perou CM, et al. High intratumoural stromal content defines reactive breast cancer as a low-risk breast cancer subtype. Clin Cancer Res 2016;22(20):5068–78.
[35] Yang L, Wang S, Lee JJ, Lee S, Lee E, Shinbrot E, et al. An enhanced genetic model of colorectal cancer progression history. Genome Biol 2019;20(1):168.
[36] Rückert F WK, Aust D, Hering S, Saeger H-D, Grützmann R, Pilarsky C. Establishment and characterization of six primary pancreatic cancer cell lines. Austin J Cancer Clin Res 2015;2(7).
[37] Kim MJ, Kim MS, Kim SJ, An S, Park J, Park H, et al. Establishment and characterization of 6 novel patient-derived primary pancreatic ductal adenocarcinoma cell lines from Korean pancreatic cancer patients. Cancer Cell Int 2017;17:47.
[38] Knudsen ES, Balaji U, Mannakee B, Vail P, Eslinger C, Moxom C, et al. Pancreatic cancer cell lines as patient-derived avatars: genetic characterisation and functional utility. Gut 2018;67(3):508–20.
[39] Curry EL, Moad M, Robson CN, Heer R. Using induced pluripotent stem cells as a tool for modelling carcinogenesis. World J Stem Cells 2015;7(2):461–9.
[40] Seki T, Fukuda K. Methods of induced pluripotent stem cells for clinical application. World J Stem Cells 2015;7(1):116–25.
[41] Boj SF, Hwang CI, Baker LA, Chio II, Engle DD, Corbo V, et al. Organoid models of human and mouse ductal pancreatic cancer. Cell 2015;160(1-2):324–38.
[42] Saito Y, Muramatsu T, Kanai Y, Ojima H, Sukeda A, Hiraoka N, et al. Establishment of patient-derived organoids and drug screening for biliary tract carcinoma. Cell Rep 2019;27(4):1265–76.
[43] Loomans CJM, Williams Giuliani N, Balak J, Ringnalda F, van Gurp L, Huch M, et al. Expansion of adult human pancreatic tissue yields organoids harboring progenitor cells with endocrine differentiation potential. Stem Cell Reports 2018;10(3):712–24.
[44] Tiriac H, Belleau P, Engle DD, Plenker D, Deschenes A, Somerville TDD, et al. Organoid profiling identifies common responders to chemotherapy in pancreatic cancer. Cancer Discov 2018;8(9):1112–29.
[45] Timofeeva OA, Palechor-Ceron N, Li G, Yuan H, Krawczyk E, Zhong X, et al. Conditionally reprogrammed normal and primary tumour prostate epithelial cells: a novel patient-derived cell model for studies of human prostate cancer. Oncotarget 2016.
[46] Beglyarova N, Banina E, Zhou Y, Mukhamadeeva R, Andrianov G, Bobrov E, et al. Screening of conditionally reprogrammed patient-derived carcinoma cells identifies ERCC3-MYC interactions as a target in pancreatic cancer. Clin Cancer Res 2016;22(24):6153–63.
[47] Crystal AS, Shaw AT, Sequist LV, Friboulet L, Niederst MJ, Lockerman EL, et al. Patient-derived models of acquired resistance can identify effective drug combinations for cancer. Science 2014;346(6216):1480–6.
[48] Hayashi H, Kohno T, Ueno H, Hiraoka N, Kondo S, Saito M, et al. Utility of assessing the number of mutated KRAS, CDKN2A, TP53, and SMAD4 genes using a targeted deep sequencing assay as a prognostic biomarker for pancreatic cancer. Pancreas 2017;46(3):335–40.
[49] Parasido E, Avetian GS, Naeem A, Graham G, Pishvaian M, Glasgow E, et al. The sustained induction of c-MYC drives nab-paclitaxel resistance in primary pancreatic ductal carcinoma cells. Mol Cancer Res 2019;17(9):1815–27.
[50] Tiriac H, Bucobo JC, Tzimas D, Grewel S, Lacomb JF, Rowehl LM, et al. Successful creation of pancreatic cancer organoids by means of EUS-guided fine-needle biopsy sampling for personalized cancer treatment. Gastrointest Endosc 2018;87(6):1474–80.
[51] Frappart PO, Hofmann TG. Pancreatic ductal adenocarcinoma (PDAC) organoids: the shining light at the end of the tunnel for drug response prediction and personalized medicine. Cancers (Basel) 2020;12(10).
[52] Palechor-Ceron N, Krawczyk E, Dakic A, Simic V, Yuan H, Blancato J, et al. Conditional reprogramming for patient-derived cancer models and next-generation living biobanks. Cells 2019;8(11):1327.
[53] Noll EM, Eisen C, Stenzinger A, Espinet E, Muckenhuber A, Klein C, et al. CYP3A5 mediates basal and acquired therapy resistance in different subtypes of pancreatic ductal adenocarcinoma. Nat Med 2016;22(3):278–87.
[54] Waddell N, Pajic M, Patch AM, Chang DK, Kassahn KS, Bailey P, et al. Whole genomes redefine the mutational landscape of pancreatic cancer. Nature 2015;518(7540):495–501.
[55] Biankin AV, Waddell N, Kassahn KS, Gingras MC, Muthuswamy LB, Johns AL, et al. Pancreatic cancer genomes reveal aberrations in axon guidance pathway genes. Nature 2012;491(7424):399–405.
[56] Bailey P, Chang DK, Nones K, Johns AL, Patch AM, Gingras MC, et al. Genomic analyses identify molecular subtypes of pancreatic cancer. Nature 2016;531(7592):47–52.

[57] Mardis ER. Applying next-generation sequencing to pancreatic cancer treatment. Nat Rev Gastroenterol Hepatol 2012;9(8):477–86.
[58] Chantrill LA, Nagrial AM, Watson C, Johns AL, Martyn-Smith M, Simpson S, et al. Precision medicine for advanced pancreas cancer: the individualized molecular pancreatic cancer therapy (IMPaCT) trial. Clin Cancer Res 2015;21(9):2029–37.
[59] Casey G, Conti D, Haile R, Duggan D. Next generation sequencing and a new era of medicine. Gut 2013;62(6):920–32.
[60] Hara T, Ikebe D, Odaka A, Sudo K, Nakamura K, Yamamoto H, et al. Preoperative histological subtype classification of intraductal papillary mucinous neoplasms (IPMN) by pancreatic juice cytology with MUC stain. Ann Surg 2013;257 (6):1103–11.
[61] Notta F, Chan-Seng-Yue M, Lemire M, Li Y, Wilson GW, Connor AA, et al. A renewed model of pancreatic cancer evolution based on genomic rearrangement patterns. Nature 2016;538(7625):378–82.
[62] Seino T, Kawasaki S, Shimokawa M, Tamagawa H, Toshimitsu K, Fujii M, et al. Human pancreatic tumour organoids reveal loss of stem cell niche factor dependence during disease progression. Cell Stem Cell 2018;22(3):454–67.
[63] Yan HHN, Siu HC, Law S, Ho SL, Yue SSK, Tsui WY, et al. A comprehensive human gastric cancer organoid biobank captures tumour subtype heterogeneity and enables therapeutic screening. Cell Stem Cell 2018;23(6):882–97.
[64] D'Agosto S, Lupo F, Corbo V. Generation of pancreatic organoid-derived isografts. STAR Protocols 2020;1(2):100047.
[65] Koledova Z, Lu P. A 3D fibroblast-epithelium co-culture model for understanding microenvironmental role in branching morphogenesis of the mammary gland. Methods Mol Biol 2017;1501:217–31.
[66] Nakamura H, Sugano M, Miyashita T, Hashimoto H, Ochiai A, Suzuki K, et al. Organoid culture containing cancer cells and stromal cells reveals that podoplanin-positive cancer-associated fibroblasts enhance proliferation of lung cancer cells. Lung Cancer 2019;134:100–7.
[67] Dijkstra KK, Cattaneo CM, Weeber F, Chalabi M, van de Haar J, Fanchi LF, et al. Generation of tumour-reactive T cells by co-culture of peripheral blood lymphocytes and tumour organoids. Cell 2018;174(6):1586–98 e12.
[68] Neal JT, Li X, Zhu J, Giangarra V, Grzeskowiak CL, Ju J, et al. Organoid modeling of the tumour immune microenvironment. Cell 2018;175(7):1972–88 e16.